

Effects of a low amount of C on the phase transformations in the AlN–Al₂O₃ pseudo-binary system

P. Tabary^{a,b}, C. Servant^{a,*}, J.A. Alary^b

^aLaboratoire de Métallurgie Structurale, URA CNRS 1107, Université de Paris-Sud, 91405 Orsay-Cedex, France

^bSociété Pechiney Electrometallurgie, Usine de Chedde, 74000 Le Fayet, France

Received 16 December 1999; received in revised form 4 April 2000; accepted 8 April 2000

Abstract

The effects of a low amount of C on the phase transformations in the AlN–Al₂O₃ pseudo-binary system are reported in samples having an AlN content in mol% ranging between 44 and about 0. Various complementary experimental techniques were used to determine the nature of the phase equilibria. Carbon is embedded in the components of three eutectics as a function of the average chemical composition of the sample in AlN. In two of them, a component belonging to the quaternary system Al–O–N–C and having a wide composition range was found. Its X-ray and neutron diffraction spectra are well refined with a hexagonal crystalline structure. © 2000 Elsevier Science Ltd. All rights reserved.

Keywords: AlN–Al₂O₃; Carbon; Phase equilibria; Phase transformations

1. Introduction

The Alons, compounds of Al, N and O in the AlN–Al₂O₃ pseudo-binary section are used as abrasive materials. We performed, recently, the crystalline structures of the ϕ' and δ phases by X-ray and neutron diffractions^{1,2} and high resolution transmission electron microscopy.³ The nature of the phase equilibria, temperature and composition range and coherence degree of the different phases submitted to different thermal treatments were also determined, in order to understand their transformations⁴, and a thermodynamic assessment of the system was made.⁵

The Alons elaborated by the Pechiney-Electrometallurgie Society contain three main impurities: intentional carbon, and unintentional silicon and iron.

Silicon and iron are introduced during the different steps of the elaboration (grinding, mixing and melting). With the elements Al, O, N, silicon forms quaternary phases named sialons. In fact, the polytype phases of the ternary system Al–O–N have an extension in the quaternary system Al–O–N–Si. We have determined that the two elements Si and Fe are present in general in

the final products as metallic precipitates such as: Si, Fe or belonging to the metallic binary systems Fe–Si, Fe–Al, Al–Si or ternary system Al–Fe–Si. They are not involved in the melting process of the Alons.

Carbon is introduced during the melting process of the elaboration in the arc furnace. In fact, in the bottom of the furnace, pieces of carbon are put in, in order to facilitate the starting of the melting. In addition, the tip of the carbon electrodes corrode during the melting and carbon pieces fall into the melting bath. The total weight amount of carbon is about 0.5 wt.% (that is about 100 g by melting of a pancake of 20 kg) and varies moderately from one melting to another one.

2. Experimental

The chemical composition of the samples studied are listed in the Table 1.

The samples were studied by several characterization techniques: X-ray (Cu $K_{\alpha 1}$ radiation), neutron ($\lambda = 2.466$ Å) diffractions and optical (OM), scanning electron (SEM) microscopies and electron microprobe analysis. By SEM, the two types of contrast (chemical and topological) are the best by using back-scattered electrons. In the case of the chemical contrast, the grey level

* Corresponding author. Fax: +33-1-6915-7833.

E-mail address: colette.servant@metal.u-psud.fr (C. Servant).

is inversely proportional to \bar{Z}_{vol} (average volume number) equal to:

$$\bar{Z}_{\text{vol}} = \frac{\rho}{\bar{M}_{\text{at}}} \bar{Z}_{\text{at}} \quad (1)$$

with \bar{Z}_{at} , and \bar{M}_{at} , respectively the average atomic number and mass of the phase and ρ , its volume mass (g cm^{-3}). Theoretically, two phases having $\Delta\bar{Z}_{\text{vol}} \sim 1\%$ can be separated. We calculated $\bar{Z}_{\text{at}}(\text{Al}_2\text{O}_3) = \bar{Z}_{\text{at}}(\text{AlN}) = \bar{Z}_{\text{at}}(\text{Al}_4\text{C}_3) = 10 e^-$ and $\bar{M}_{\text{at}}(\text{Al}_2\text{O}_3) \sim \bar{M}_{\text{at}}(\text{AlN}) \sim \bar{M}_{\text{at}}(\text{Al}_4\text{C}_3) \sim 20.5 \text{ g}$. Therefore \bar{Z}_{at} and \bar{M}_{at} are practically constant along the pseudo-ternary section $\text{Al}_2\text{O}_3\text{--AlN--Al}_4\text{C}_3$ and \bar{Z}_{vol} is directly related to the volume mass of the phases: lower are these data, darker appears the phase by using the SEM. So the contrast of the phase becomes lighter from $\text{Al}_4\text{O}_4\text{C}$ ($\rho = 2.72$), Al_4C_3 or Al_2OC ($\rho = 3$), “AIONC” ($\rho = 3.15$), AlN ($\rho = 3.26$), $\gamma\text{-AlON}$ ($\rho = 3.68$), $\phi'\text{-AlON}$, $\delta\text{-AlON}$ to $\alpha\text{-Al}_2\text{O}_3$ ($\rho = 3.97$). The main phases observed in the different samples after slow or fast cooling are indicated in the Table 2, as well as their volume fraction (in %).

R_c noted slow and fast was respectively equal to 15 and 500–1000 K min^{-1} . In the case of the fast cooling of the liquid on a metallic sheet, the C composition of the liquid is lower, see Table 6.

The phase transformations were followed by scanning differential thermal analysis in a device type SETARAM-TAG 24. The heating and cooling rates were equal to 10 K min^{-1} . The atmosphere used was argon at $\sim 1 \text{ atm}$. Pure corundum was used as a standard for the melting temperatures (2327 K).

The neutron diffraction spectra were treated with the profile refinement method of Rietveld⁶ with the help of the FullProf software of Rodriguez.⁷

3. Results and discussion

In the samples, the carbon is present under two forms:

- (i) either as graphite which does not react during the melting;
- (ii) or embedded in precipitates belonging to the quaternary system Al--O--N--C . As for the ternary system Al--O--N , the four elements Al--O--N--C can only exist in the solid state as combination of the neutral simple elements such as: Al_2O_3 , AlN and Al_4C_3 , so in a pseudo-ternary system. In this system, the phases containing carbon are listed in the Table 3.

The phase diagram $\text{Al}_2\text{O}_3\text{--Al}_4\text{C}_3$ plotted in the Fig. 1 has been studied by Foster et al.⁸ The presence of an eutectic $\text{Al}_2\text{O}_3\text{--Al}_4\text{O}_4\text{C}$ at the composition 90 $\text{Al}_2\text{O}_3\text{--}10 \text{ Al}_4\text{C}_3$ (in mol%), that is 4.2 wt.% of Al_4C_3 has been found. Thermodynamics of the Al--C--O system, recently assessed by Lihmann et al.¹³ shows that Al_2OC decomposes below 1710°C in good agreement with the experimental data (1715°C) of Lihmann et al.¹⁴

In the presence of AlN , this temperature becomes much lower. In fact, in the $\text{AlN--Al}_2\text{OC}$ system, studied by Kuo et al.,¹⁵ stable Al_2OC -rich precipitates were observed in a 61% $\text{AlN--}39\% \text{ Al}_2\text{OC}$ solid solution

Table 1
Composition of the samples considered in the present work

Sample no.	Chemical composition (wt.%)						Composition (mol% AlN)
	Al	O	N	C	Fe	Si	
1	56.1	38	8–8.95	0.26–0.43	0.3	0.27	43.3±2.2
2			6.38				36.3±1.8
3	55	40	4.6–5.23	0.14	0.4	0.25	29.6±1.5
4	55.2	41	4.5–4.88	0.72	0.38	0.24	28.2±1.4
5	54.4	43	3.4	0.57	0.21	0.23	21.3±1.1
6	53.7–54.3	46–44	1.6–1.5	0.35–0.15	0.14	0.1	10.55±0.5
7	53.4	45	0.5	0.94			3.5±0.2

Table 2
Main phases in the samples studied

Sample no.	Cooling rate: (R_c)	AlN/polytypes (mol%)	γ (mol%)	ϕ' (mol%)	δ (mol%)	$\alpha\text{-Al}_2\text{O}_3$ (mol%)
1	Slow	7.8 AlN + 4.2 21R	88	Traces		
4	Slow	Traces	85	10		
5	Slow		56.7	42.1		1.1
6	Slow		3.5	85.9	4.4	5.9
7	Fast and slow				84.5	15.4

Table 3
Crystalline data of phases containing carbon

Chemical formula	M/X	System	a (Å)	b (Å)	c (Å)	Space group	Ref.	ASTM
Al ₄ O ₄ C		orth.	9.23	8.64	5.77		(8)	14–630
Al ₂ OC		hex.	3.170		5.078	P6 ₃ /mmc(194)	(9)	36–148
Al ₂ OC		hex.	3.153		4.987	P6 ₃ /mmc(194)	(9)	36–149
Al ₄ C ₃		hex.	3.339		25.00	R3m(166)	(10)	35–799
Al ₅ C ₃ N	5/4	hex.	3.281		21.67	P6 ₃ mc (186)	(11)	
Al ₆ C ₃ N ₂	6/5	hex.	3.248		40.03	R3m (166)	(11)	
Al ₇ C ₃ N ₃	7/6	hex.	3.226		31.70	P6 ₃ mc (186)	(11)	
Al ₈ C ₃ N ₄	8/7	hex.	3.211		55.08	R3m (166)	(11)	
(Al ₂ OC) _(1-x) (AlN) _x Wurtzite structure	1	hex.	3.123		4.994		(12)	26–9

exposed at 1600°C for 500 h. In addition, continuous Al₂OC–AlN (2H) solid solutions were found at 1880°C in the 0–44 mol% Al₂OC range¹⁵ and at 1980°C in the 0–40 mol% range.¹⁴

The ternary system Al₂O₃–AlN–Al₄C₃ has been studied by Henry et al.¹⁶ Zambétakis¹⁷ and Lihrmann et al.¹⁸ The two first authors found the existence of the solid solution Al₂OC_(1-x)AlN_x for AlN content equal respectively to 60 and 50 mol%.

The polytypes of the pseudo-binary system Al₄C₃–AlN having the formula Al_nC₃N_{n-4} belong to the R3m space group (as well as Al₄C₃) if n is odd and P6₃mc (as well as AlN-2H) if n is even. Their formula always verifies M/X = n/(n-1), with M = n_{Al} and X = n_C + n_N.

3.1. Optical and scanning electron microscopy analysis

As a function of the composition in AlN (mol%) of the sample, the nature of the matrix is different as shown in the Table 4. The phases containing carbon are observed at the grain boundaries of this matrix with an eutectic morphology which is more or less well resolved. Three different eutectics are revealed as a function of this composition in AlN: eutectic No. 1 in the Sample 5 and eutectics No. 2 and 3 in the Sample 6, as listed in the Table 4. With the help of the OM, they appear lighter than the phases of the Al₂O₃–AlN system while by using the back-scattered electrons in SEM they appear darker. These facts indicate that their density is weaker than the ones of the phases of the AlN–Al₂O₃ system as shown in the Eq. (1). Furthermore, they appear recessed from the matrix because their hardness is probably lower.

The “AlONC” phase belongs to the Al₂O₃–AlN–Al₄C₃ pseudo-ternary system.

The mol fraction of each component of the eutectics numbered 1 and 3 has been calculated by considering ρ(“AlONC”) ~ 3.15 g cm⁻³.

The eutectic numbered 1 (Fig. 2a) is generally resolved except in some rare cases when only nodules of “AlONC” are observed. Its temperature of melting is higher than 1950°C.

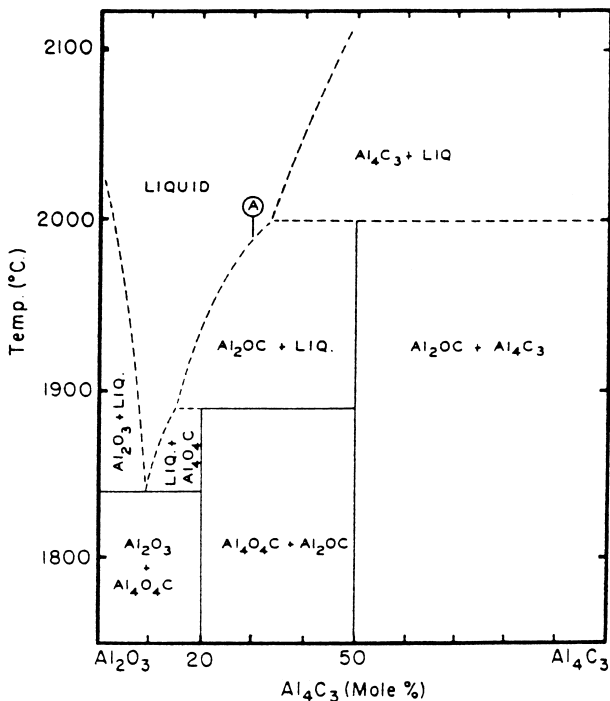


Fig. 1. Al₂O₃–Al₄C₃ pseudo-binary section from Foster et al.⁸

Table 4
Characteristics of the phases observed in Samples 5 and 6

Eutectic no.	Matrix		Components of the eutectic		
	Phases	C _{min} (AlN%)	Phase 1	Vol.%	Mol% Phase 2
1	γ, φ'	> 16	γ, φ'	40	44.5 “AlONC” (+ s.s. Al ₂ OC-AlN)
2	φ'	13 à 16	φ'	45	56 Al ₄ O ₄ C
3	φ', δ	< 13	Al ₂ O _{3z}	65	70 “AlONC” (+ s.s. Al ₂ OC-AlN)

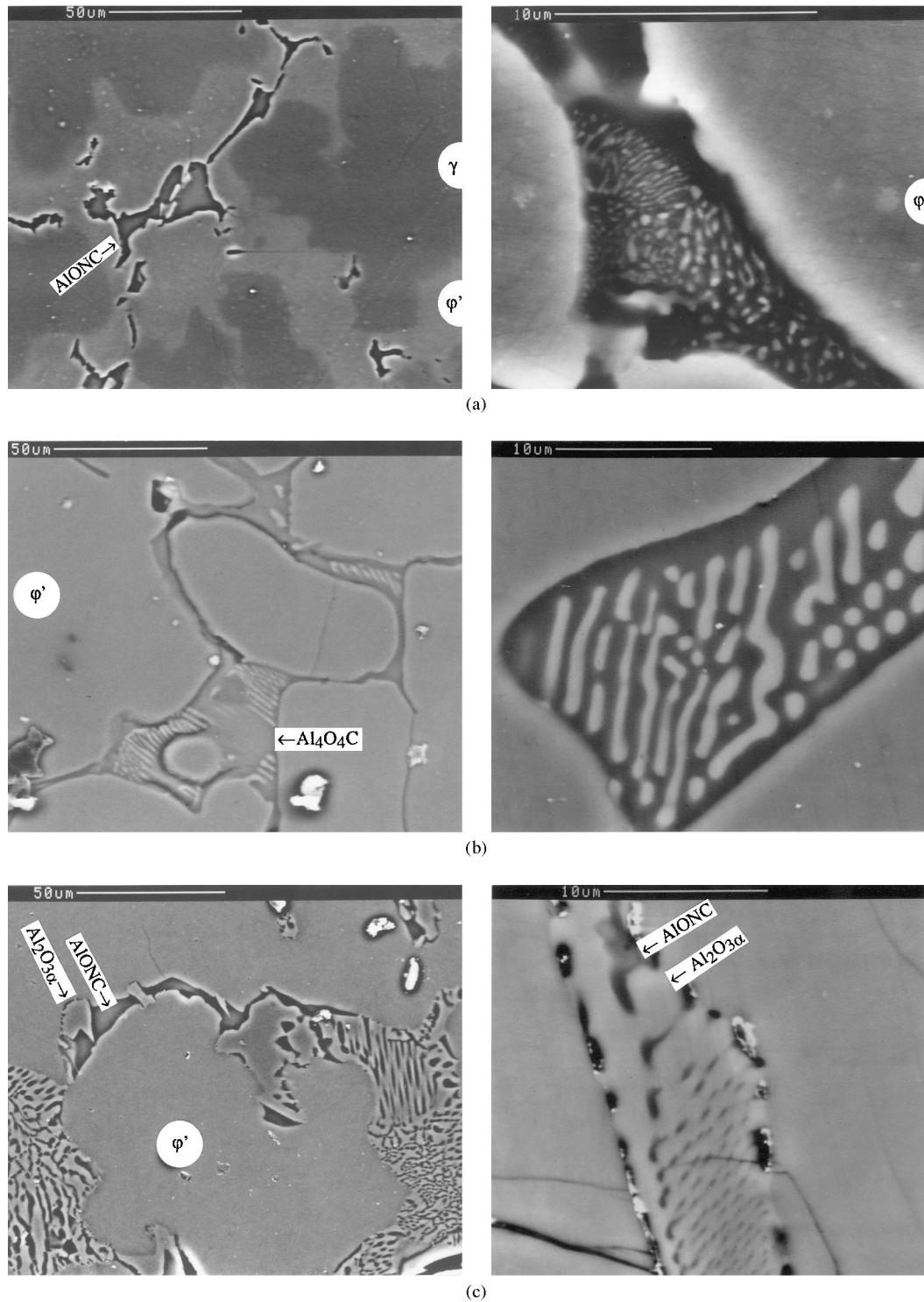


Fig. 2. Back-scattered electron micrographs of the eutectics. (a) Eutectic No. 1 (ϕ' -AlON + "AlONC") in the (ϕ' -AlON + γ -AlON) matrix of sample 5. (b) Eutectic No. 2 (ϕ' -AlON + $\text{Al}_4\text{O}_4\text{C}$) in the (ϕ' -AlON) matrix of Sample 6. (c) Eutectic No. 1 (Al_2O_3 + "AlONC") in the (ϕ' -AlON) matrix of Sample 5.

The eutectic numbered 2 presents sometimes lamella with a large size and some nodules with about a 1.5 μm interdistance, Fig. 2b.

The morphology of the eutectic numbered 3 is either lamellar with an interdistance varying from 0.45 to 1.5

μm , or with nodules of "AlONC" having a $\sim 0.8 \mu\text{m}$ interdistance, Fig. 2c. The average composition of the eutectic 3 has been confirmed with the help of the electron microprobe. On some micrographs, corundum grains are clearly observed near this eutectic.

The average composition of the eutectics numbered 1, 2 and 3 is more and more depleted in nitrogen because they precipitate in equilibrium with a matrix which is also more and more depleted in nitrogen.

3.2. Chemical, X-ray and neutron diffraction analysis

A low amount of the graphite-2H (space group $P6_3/mmc$) is detectable with the help of the neutron diffraction due to the high intensity of the (002) reflection of the graphite. The refined c parameter is equal to 6.728 Å against data found in the literature such as: $(a,c) = (2.464 \text{ Å}, 6.711 \text{ Å})$ ¹⁹ and $(a,c) = (2.470 \text{ Å}, 6.724 \text{ Å})$ ²⁰. The different techniques of analysis allow to determine the weight fractions listed in the Table 5.

In the Sample 7, slowly cooled, noted with the symbol (*) in Table 5, the carbon is present both as a graphite and as precipitates contrary to the Sample 7 fastly cooled and noted by the symbol (**) in the same table. This difference is certainly due to the process of cooling on a metallic sheet. In fact, only the liquid phase situated in the upper part of the furnace and which contains a lower amount in carbon is then gathered.

The difference between the wt.% C determined by chemical analysis and measured by neutron diffraction gives the wt.% C dissolved in the liquid phase. This dissolution is complete in Sample 5, partial in Sample 6 and practically equal to zero in Sample 1. This can be explained by the transformation more or less fast in the liquid state when the melting starts. The average total weight fraction of carbon (~0.5 wt.%) in the samples corresponds in the ternary system $Al_2O_3-AlN-Al_4C_3$ to 1.25 mol% of Al_4C_3 . As an example, it can be noted that 0.5 wt.% of dissolved C corresponds to 6.5 vol.% of “AIONC” and 0.1 wt.% of C to 1.5 vol.% of Al_4O_4C .

3.3. Study of “AIONC”

3.3.1. Composition (microprobe)

As the samples analysed with the help of the microprobe are in general covered with a thin sheet of carbon, the weight fraction of carbon is determined as the following difference: $wt.\% C = 100 - (wt.\% Al + wt.\% O + wt.\% N)$. This equation was first used without

correction. As the charge balance showed a shift corresponding to an excess of carbon, the coefficients of Al, O and N have been verified. It seems that the real curling on these phases is slightly lower than the one on the matrix, maybe due to the recessed morphology of the precipitates. By using a sum of the weight fractions equal to 98.5 instead of 100, a charge balance equal to zero was found.

The mol composition of the “AIONC” phase linearly varies between P_1 [25% Al_2O_3 –75% AlN] and P_2 [60% Al_2O_3 –20% AlN –20% Al_4C_3], Fig. 3. The intersection point of this straight line with the $Al_2O_3-Al_4C_3$ section would be at 26.5 mol% Al_4C_3 , which does not correspond to a compound cited in the literature: in fact, Al_4O_4C is found at 20 mol% Al_4C_3 and Al_2OC at 50 mol% Al_4C_3 . Three domains can be distinguished in the mole% AlN composition range:

The general formula of the polytypes in the $AlN-Al_2O_3$ pseudo-binary section is $Al_nO_3N_{(n-2)}$. In the $Al_2O_3-Al_4C_3$ pseudo-binary section, this formula becomes: $Al_{(x+4)}O_{(1.5x)}C_3$. When x is respectively equal to 8, 6, 5, 4.4 and 4 the ratio $M/X = n/n+1$ with $M = (n_{Al})$ and $X = (n_O + n_C)$ is equal to 4/5, 5/6, 6/7, 7/8 and 8/9. It must be noted that the compounds of the

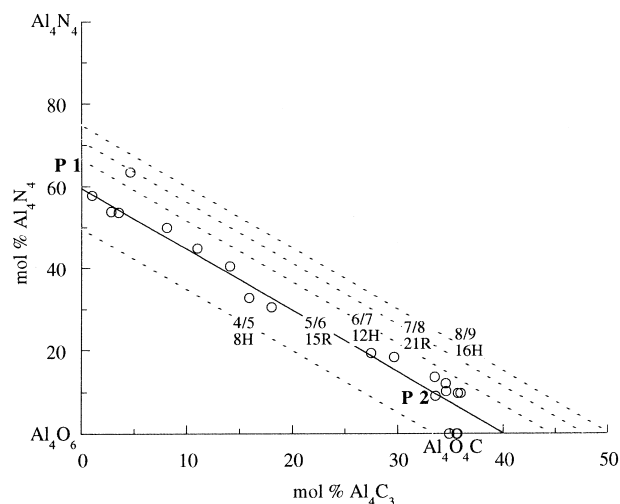


Fig. 3. Composition range of the “AIONC” phase in the pseudo-ternary section $Al_4O_6-Al_4N_4-Al_4C_3$.

Table 5
Weight fractions of C measured in the different samples

Sample no.	1	4	5	6	7(*)	7(**)
Total wt.% C (measured by chemical analysis)	0.26–0.43	0.72	0.57	0.35–0.15	0.94	< 0.94
wt.% C_{2H} (measured by neutron diffraction)	0.42	— ^a	0.07	0.29–0.21	—	0.06 (**)
Detected phase by X-ray and neutron diffractions	—	“AIONC”	“AIONC”	Al_4O_4C	—	—
Vol.% of precipitates detected by OM	0.0	—	~4	1 to 2	—	0.0

^a Means not determined.

$\text{Al}_2\text{O}_3\text{--Al}_4\text{C}_3$ pseudo-binary section have not a polytype structure as R3m or P6₃mc (see Table 3).

In order to plot the pseudo-ternary system $\text{Al}_2\text{O}_3\text{--AlN--Al}_4\text{C}_3$, it is interesting to use the Al_4O_6 , Al_4N_4 and Al_4C_3 compounds. In fact, $M = n_{\text{Al}}$ is then a constant for the whole diagram and $X = (n_{\text{O}} + n_{\text{C}} + n_{\text{N}})$. It is well known that the composition of the polytypes verifies the relation $M/X = \text{constant}$ with $X = M + 1$ when they present a domain of solid solution. In Fig. 3, the parallel straight lines having the equation $M/X = 4/5, 5/6, 6/7, 7/8, 8/9$ (which corresponds respectively to the structures of the polytypes 8H, 15R, 12H, 21R, 16H) as well as the $\text{Al}_4\text{O}_4\text{C}$ compound (which has not a polytype structure) have been plotted, see the Table 7. As an example, the intersection of the straight line (slope 5/6) representing the possible composition range of the 15R polytype ($\text{Al}_5\text{O}_3\text{N}_{(5-2)} = 3\text{AlN} + \text{Al}_2\text{O}_3$) in the $\text{AlN--Al}_2\text{O}_3$ pseudo-binary section is situated at (3/4) mol AlN, while in the $\text{Al}_4\text{N}_4\text{--Al}_4\text{O}_6$ pseudo-binary section ($\text{Al}_5\text{O}_3\text{N}_{(5-2)} = 3/4 \text{Al}_4\text{N}_4 + 1/2 \text{Al}_4\text{O}_6$), it is situated at $(3/4)/((3/4) + (1/2))$ that is 0.6 mol Al_4N_4 . It can be noted that the domain of composition of the “AIONC” compound (noted with empty circles) is set in a parallel direction to these straight lines and is very near the one of the 15R polytype. The 15R polytype is not stable in the $\text{Al}_2\text{O}_3\text{--AlN}$ pseudo-binary system but is observed in the $\text{Al}_2\text{O}_3\text{--AlN--SiO}_2\text{--Si}_3\text{N}_4$ pseudo-ternary system.²¹ Furthermore it can be noted that the solid solution $\text{Al}_2\text{OC}_{(1-x)}\text{AlN}_x$ corresponds to a compound of the preceding type with a structure 2H and $M/X = 1$ (limite case of the polytypes with $X = M + 1$, M and X tending to infinity, see Table 3).

Table 6
Characteristic of the eutectics numbered 1 and 3

Eutectic no.	Matrix	%AlN (“AIONC”)
1	γ	> 55
1	$\gamma + \phi'$	35–55
1	$\gamma + \phi'$	20–35
3	ϕ', δ	20–35

Table 7

Coordinates of the intersections (with the axis of pseudo-binary sections differently plotted) of the straight lines corresponding to the possible composition range of some polytypes $2n\text{H}$ and $3n\text{R}$

$M/X = n/n + 1$	Polytype $2n\text{H}$ or $3n\text{R}$	Section $\text{AlN--Al}_2\text{O}_3$	Section $\text{Al}_4\text{N}_4\text{--Al}_4\text{O}_6$	Section $\text{Al}_2\text{O}_3\text{--Al}_4\text{C}_3$	Section $\text{Al}_4\text{O}_6\text{--Al}_4\text{C}_3$
		Formula — mol% AlN	Mol% Al_4N_4	Formula — mol% Al_4C_3	Mol% Al_4C_3
4/5	8H	$\text{Al}_4\text{O}_3\text{N}_2$: 66.67	50	$\text{Al}_{12}\text{O}_{12}\text{C}_3 = \text{Al}_4\text{O}_4\text{C}$: 20.0	33.33
5/6	15R	$\text{Al}_5\text{O}_3\text{N}_3$: 75	60 (P1)	$\text{Al}_{10}\text{O}_9\text{C}_3$: 25.0	40.0
6/7	12H	$\text{Al}_6\text{O}_3\text{N}_4$: 80	66.67	$\text{Al}_9\text{O}_{7.5}\text{C}_3$: 28.57	44.44
7/8	21R	$\text{Al}_7\text{O}_3\text{N}_5$: 83.33	71.38	$\text{Al}_{8.4}\text{O}_{6.6}\text{C}_3$: 31.25	47.61
8/9	16H	$\text{Al}_8\text{O}_3\text{N}_6$: 85.71	75	$\text{Al}_8\text{O}_6\text{C}_3$: 33.33	50.0
				$\text{Al}_6\text{O}_3\text{C}_3 = \text{Al}_2\text{OC}$: 50	66.67

3.4. Crystalline cell (X-ray and neutron diffractions)

With the help of the X-ray diffraction, in Samples 4 and 5, some reflections of phases containing carbon (in particular the interdistances $d = 1.575$ and 2.734 Å) are observed. Furthermore, the refinement of the neutron diffraction spectrum of Sample 1 allowed the determination of the reflections of AlN in particular: $(002)_{\text{AlN}}$ ($d_1 = 2.490$ Å) and $(100)_{\text{AlN}}$ ($d_2 = 2.695$ Å), see Fig. 4. In the case of Sample 4, AlN is also present but in addition there are peaks preceding the AlN reflections which are well taken into account by considering a phase containing carbon having a hexagonal cell with parameters: $(\mathbf{a}, \mathbf{c}) = (3.153$ Å, 4.980 Å) and interdistance of (hkl) planes: $d((110), (002), (100)) = (1.576$ Å, 2.490 Å, 2.731 Å). These parameters are not consistent with those of the $\text{Al}_2\text{OC}_{(1-x)}\text{AlN}_x$ solid solution but are very near those of a phase having the composition Al_2OC (distinct of the “classical” Al_2OC phase), and identified by Fujishige et al.,⁹ and having the parameters: $(\mathbf{a}, \mathbf{c}) = (3.153$ Å, 4.987 Å).

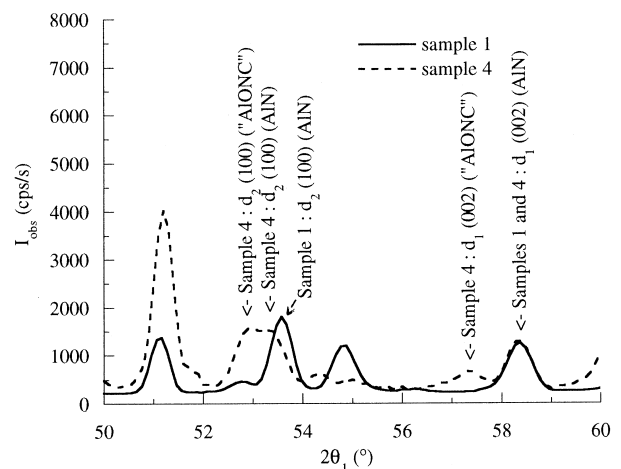


Fig. 4. Neutron diffraction spectra of Samples 1 and 4. Comparative intensities of the (002) and (100) reflections of AlN and “AIONC”.

4. Conclusion

Due to the presence of impurities in the start material, precipitation of intermetallic phases (specially phases containing carbon) occurs at the grain-boundaries of the matrix of the samples. Three different eutectics can precipitate as a function of the average chemical composition of C in the sample. The chemical composition of the components of each eutectic has been determined.

Two of these eutectic contain a phase belonging to the quaternary system Al–O–N–C. This phase has a wide homogeneity range. From the data determined with the help of the X-ray and neutron diffraction spectra, we have proposed a hexagonal crystalline cell for this phase.

Acknowledgements

The authors are indebted to Dr. G. André du Laboratoire Léon Brillouin du Centre d'Etudes de Saclay for neutron experiments.

References

1. Tabary, P. and Servant, C., Crystalline and microstructure study of the AlN–Al₂O₃ section in the Al–N–O system, I. Polytypes and γ -Alon spinel phase. *J. Appl. Cryst.*, 1999, **32**, 241–252.
2. Tabary, P. and Servant, C., Crystalline and microstructure study of the AlN–Al₂O₃ section in the Al–N–O system, II. ϕ' and δ -Alon spinel phase. *J. Appl. Cryst.*, 1999, **32**, 253–272.
3. Tabary, P., Servant, C. and Guymont, M., High resolution transmission electron microscopy study of the ϕ' and δ -Alon spinel phases of the pseudo-binary section AlN–Al₂O₃. *J. Appl. Cryst.*, 1999, **32**(4), 755–790.
4. Tabary, P., Servant, C. and Alary, J. A. Microstructure and phase transformations in the AlN–Al₂O₃ pseudo-binary system. *J. Eur. Ceram. Soc.*, 2000, **20**, 913–926.
5. Tabary, P. and Servant, C., Thermodynamic reassessment of the AlN–Al₂O₃ system. *Calphad*, 1998, **22**(2), 179–201.
6. Rietveld, H. M., A profile refinement method for nuclear and magnetic structures. *J. Appl. Cryst.*, 1969, **2**, 65–71.
7. Rodríguez, J., *Manual of the Computer Program Fullprof*. Laboratoire Léon Brillouin, Saclay, France, 1994.
8. Foster, L. M., Long, G. and Hunter, M. S., Reactions between aluminum oxide and carbon — the Al₂O₃–Al₄C₃ phase diagram. *J. Am. Ceram. Soc.*, 1956, **39**(1), 1–11.
9. Fujishige, M., Aluminium oxide carbide, Al₂OC. *J. Nat. Chem. Labor. Ind.*, 1982, **77**, 325.
10. Nat. Bur. Stand. (US), Aluminium carbide Al₄C₃. *Monograph*, 1984, **21**.
11. Jeffrey, G. A. and Wu, V. Y., The structures of the aluminum carbonitride. *Acta Cryst.*, 1963, **16**, 559.
12. Zaretskaya, L., *Inorg. Materials*, 1972, **8**, 70–72.
13. Lihmann, J. M., Tirllocq, J., Descamps, A. and Cambier, F., Thermodynamics of the Al–C–O system and properties of SiC–AlN–Al₂OC composites. *J. Eur. Ceram. Soc.*, 1999, **19**(16), 2781–2787.
14. Lihmann, J. M., Zambétakis, T. and Daire, M., High temperature behavior of the aluminium oxycarbide Al₂OC in the system Al₂O₃–Al₄C₃ and with additions of aluminium nitride. *J. Am. Ceram. Soc.*, 1989, **72**(9), 1704–1709.
15. Kuo, S. Y. and Virkar, A. V., Phase equilibria and phase transformations in the AlN–Al₂OC pseudo-binary system. *J. Am. Ceram. Soc.*, 1989, **72**(4), 540–550.
16. Henry, J. L., Russel, J. H. and Kelly, H. J., The system Al₄C₃–AlN–Al₂O₃. *US Bur. Mines, Report of Investigations*, No. 7320, Nov. 1969.
17. Zambétakis, T., Préparation et propriétés de céramiques composites dans les systèmes C–Al–O–N et Zr–Al–O–C: application à l'abrasion, Université L. Pasteur, 1985.
18. Lihmann, J. M., Nouvelles céramiques fondues dans le système C–Al–O–N; examen de leur aptitude à l'abrasion, Université L. Pasteur, 1982.
19. Villars, P. and Calvet, L. D., *Pearson's Handbook of Crystallographic Data for Intermetallic Phases*, 1986, **2**, 1502.
20. Sanc, I. Polytechnica. Foreign Trade corporation, Panska, Czechoslovakia. Joint Committee on Powder Diffraction Standards, Grant-in-Air Report, No. 41-1487, 1990.
21. Jack, K. H., Review: sialons and related nitrogen ceramics. *J. Mater. Sci.*, 1976, **11**, 1135–1158.